JOURNAL OF MATERIALS SCIENCE 35 (2000) 2245–2253

Effects of aging temperature on the microstructure and mechanical properties of 1.8Cu-7.3Ni-15.9Cr-1.2Mo-low C, N martensitic precipitation hardening stainless steel

H. NAKAGAWA*, T. MIYAZAKI
Department of Materials Science and Engineering, Nagoya Institute of Technology, Gokiso-cho Showa-ku Nagoya 466-8555, Japan

H. YOKOTA
Assistant Manager, Development Div. No. 1, AICHI STEEL CORPORATION, 1 Wano-wari Arao-machi Tokai 476-8666, Japan

The effects of aging temperature on the microstructure and mechanical properties of a newly designed martensitic precipitation hardening stainless steel, which is 1.8Cu-15.9Cr-7.3Ni-1.2Mo-low C, N steel, for improving the toughness, ductility and corrosion resistance of stainless steel of 1000 MPa grade tensile strength were experimentally investigated. The specimen aged at 753 K for 14.4 ks has a typical lath martensitic structure with about 12% interlath austenite, while the specimens aged at 813 K and 853 K for 14.4 ks have the lamellar duplex microstructure of the reverted austenite and the aging hardened martensite. The formation process of reverted austenite is controlled by diffusion of Ni in martensite. The mean size of precipitates which are enriched with Cu increases with rising aging temperature, however, it is about 30 nm even after aging at 853 K for 14.4 ks. The specimens aged at 813 K and 853 K for 14.4 ks, in which the reversion of martensite to austenite is observed, have the excellent combinations of strength, ductility and toughness.

1. Introduction

Martensitic precipitation hardening stainless steels such as 17-4 PH and PH 13-8 Mo stainless steels are widely utilized because of their high strength with reasonable toughness, ductility and corrosion resistance [1]. However, those properties and their combinations are not always satisfactory to their users, and the improvement of those properties have been also expected.

From these circumstances, we have newly designed a martensitic precipitation hardening stainless steel, which is 1.8Cu-15.9Cr-7.3Ni-1.2Mo-low C, N steel, for improving the toughness, ductility and corrosion resistance of stainless steel of 1000 MPa grade tensile strength [2]. The main features of this steel are as follows: (1) About 10% austenite, γ, remains after solution treatment. (2) C and N contents are lowered for controlling the precipitation of carbides and nitrides. (3) 1.2mass%Mo is added for high corrosion resistance. (4) 1.8mass%Cu is added as a element for precipitation hardening. The purpose of this study was to clarify the effects of aging temperature on the microstructure and mechanical properties of this newly designed martensitic precipitation hardening stainless steel.

2. Specimen and experimental procedure

2.1. Specimen

The Chemical composition of the steel used in the present work is shown in Table I. Fig. 1 shows the phase diagram calculated by the Thermo-Calc software [3]. When compared to Fe-Cr-Ni ternary phase diagram [4], Fig. 1 is found to have Laves phase and ε-Cu phase regions as a result of Mo and Cu additions, respectively.

The steel was melted by using the multistage steelmaking process and then produced as rolled bars 80 mm and 67.5 mm in diameter by AICHI STEEL CORPORATION for minimizing non-metallic inclusions and impurities. Then the rolled bars 80 mm in diameter were hot forged as bars 15 mm in diameter. The rolled bars 67.5 mm in diameter were used for the evaluation of mechanical properties, while the forged bars were used for other examinations. These rolled and forged bars were solution treated at 1273 K for 1.2 ks, air cooled to room temperature. Subsequently these bars

* Author to whom all correspondence should be addressed.

TABLE I Chemical composition of the present steel (mass%)

C	Cu	Ni	Cr	Mo	Nb	N	Fe
0.008	1.78	7.29	15.91	1.16	0.08	0.017	Bal.

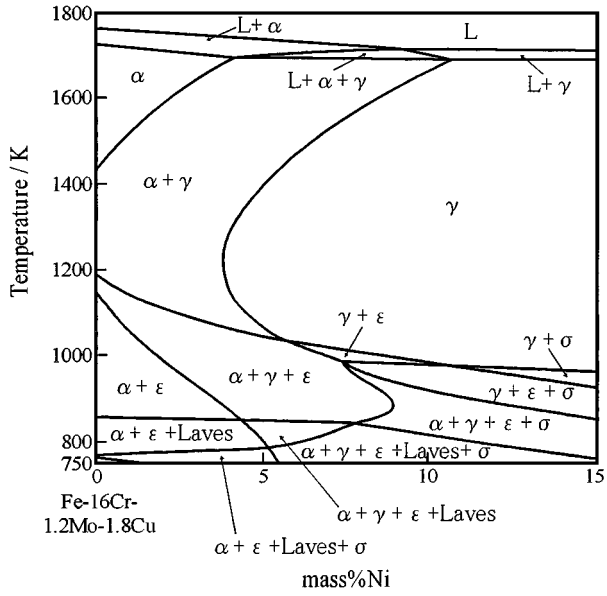

Figure 1 Phase diagram calculated by the Thermo-Calc software.

were aged at different temperatures in the range 653 K–953 K for various durations and then air cooled to room temperature.

2.2. Experimental procedure

The heat treated bars were examined by means of hardness test, X-ray diffraction technique, optical microscopy, transmission electron microscopy (TEM), and mechanical tests. The hardness tests were performed on the tester set to the Rockwell C scale. The quantitative measurements of γ were determined by X-ray diffraction technique with Cu K_α radiation in Rigaku X-ray diffractometer (Rint1100). The amounts of γ were estimated by the comparison of three peaks ($(200)_{bcc}$, $(211)_{bcc}$, $(220)_{bcc}$ and $(200)_{fcc}$, $(220)_{fcc}$, $(311)_{fcc}$) for each phase so as not to be affected by the preferred crystallographic orientation [5]. Optical microstructures were examined after etching with a reagent containing of 5 ml of hydrochloric acid, 4 g of picric acid and 100 ml of ethyl alcohol. Thin foils for transmission electron microscopy were prepared by mechanical thinning to a thickness of 0.1 mm and followed by electropolishing at 288 K in an electrolyte containing 50 ml of perchloric acid and 450 ml of acetic acid. Those thin foils were examined in a JEM 2000FX operating at 200 kV. The mechanical properties were evaluated by means of tensile test and Charpy impact test at room temperature. The tensile tests were performed on 8 mm diameter round specimens with 40 mm gauge length. The crosshead speeds were 2 mm/min in the elastic range and 5 mm/min in the plastic range. The impact tests were performed on full-size Charpy V-notch impact specimens. Fractographic features of impact specimens were examined by means of scanning electron microscopy.

3. Experimental results

3.1. Changes in hardness and amount of austenite with aging

Fig. 2 shows the variations in hardness and amount of γ with aging time at various temperatures. The hardness of solution treated specimen is found to be 26 Rockwell C hardness, and the hardness changes with aging time are found to be divided into the following three types (Fig. 2a): (1) At 653 K and 753 K, the hardness increases with aging time. (2) At 813 K and 853 K, the hardness increases at early stage and then gradually decreases with aging time. (3) At 953 K, the hardness dose not change with aging time. On the other hand, solution treated specimen is found to contain about 12% retained γ, and the changes of amount of γ with aging time are found to be divided into the following three types in the same manner as the hardness changes (Fig. 2b): (1) At 653 K and 753 K, the amount of γ dose not change with aging time. (2) At 813K and 853K, the amount of γ gradually increases with aging time. This increase may be due to the reversion of martensite to γ. (3) At 953 K, the amount of γ remarkably increases at

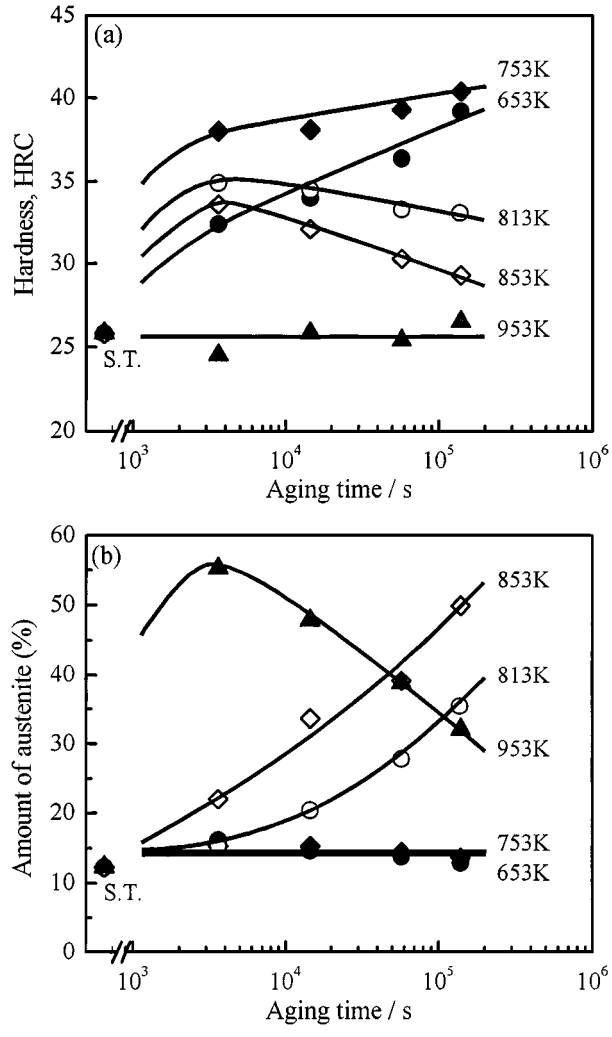

Figure 2 Variations in (a) hardness and (b) amount of austenite with aging time at various temperatures.

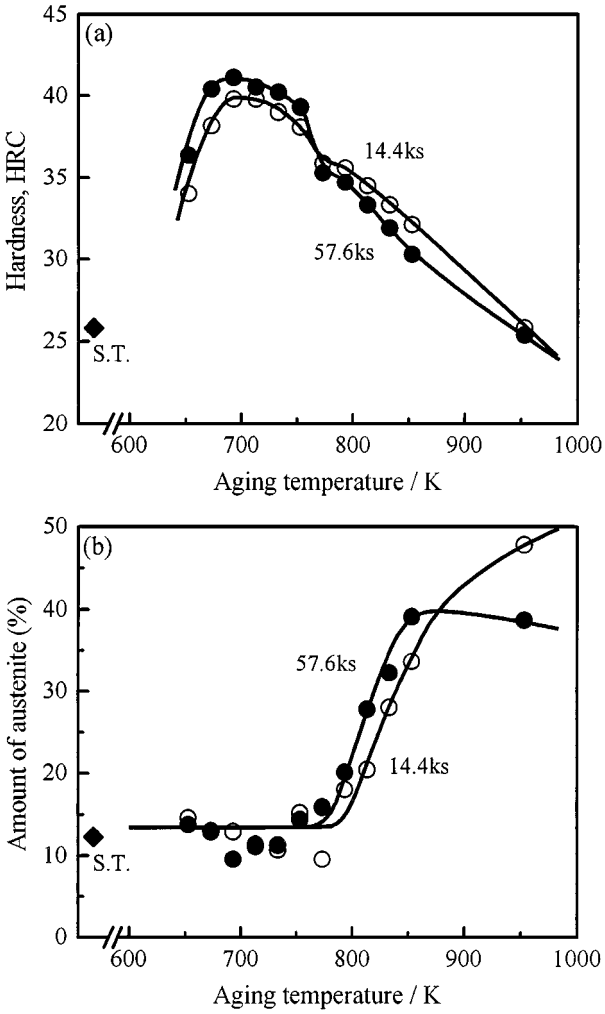

Figure 3 Variations in (a) hardness and (b) amount of austenite with aging temperature for 14.4 ks and 57.6 ks.

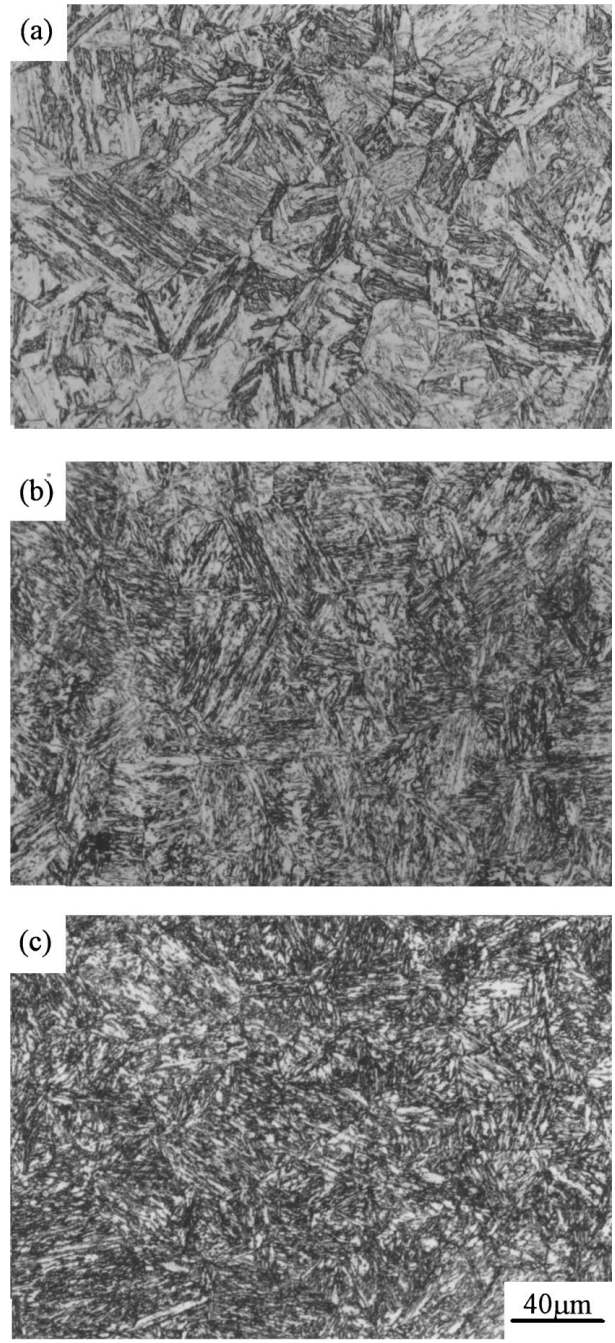

Figure 4 Optical micrographs of the specimens aged at (a) 753 K, (b) 813 K and (c) 853 K for 14.4 ks.

early stage and then linearly decreases with aging time. This decrease may be due to the partially martensitic transformation of reverted γ during cooling after aging. Consequently, the hardness changes of the present steel with aging time may depend on the balance between the softening due to the reversion and the hardening due to the precipitation. However, the reason of no hardness change on aging at 953 K is not clear.

Fig. 3 shows the variations in hardness and amount of γ with aging at various temperatures for 14.4 ks and 57.6 ks. The maximum increments of hardness are found to occur on aging at around 693 K for both aging times (Fig. 3a). Moreover, the specimens aged below 753 K are found to have a higher hardness on aging for 57.6 ks, while conversely the specimens aged above 773 K are found to have a higher hardness on aging for 14.4 ks. The reversion of martensite to γ can be found on aging above around 773 K, though there are some scattering in measured γ contents (Fig. 3b). Therefore, the deference of hardness change may depend on whether the reverted γ is formed or not.

3.2. Observation of microstructure

Fig. 4 shows the optical micrographs of the specimens aged at 753 K, 813 K and 853 K for 14.4 ks. A lath martensitic structure in a prior γ grain, whose size is about 30 μm in diameter, is resolved in the specimen aged at 753 K (Fig. 4a), while not clearly resolved in the specimens aged at 813 K (Fig. 4b) and 853 K (Fig. 4c). This difference may be due to the reversion of martensite to γ as shown in Figs 2b and 3b. The δ-ferrite which exercises harmful influence on toughness was not observed, although Fig. 1 shows that the specimen should contain the δ-ferrite after casting. Such δ-ferrite may be dissolved during the heating, rolling and forging.

Fig. 5 shows the transmission electron micrographs of the specimen aged at 753 K for 14.4 ks. The bright field image (Fig. 5a) shows the typical lath morphology of martensite containing a very high density of dislocation. The width of the laths is found to be 0.1–0.5 μm which is the same as some other experimental results

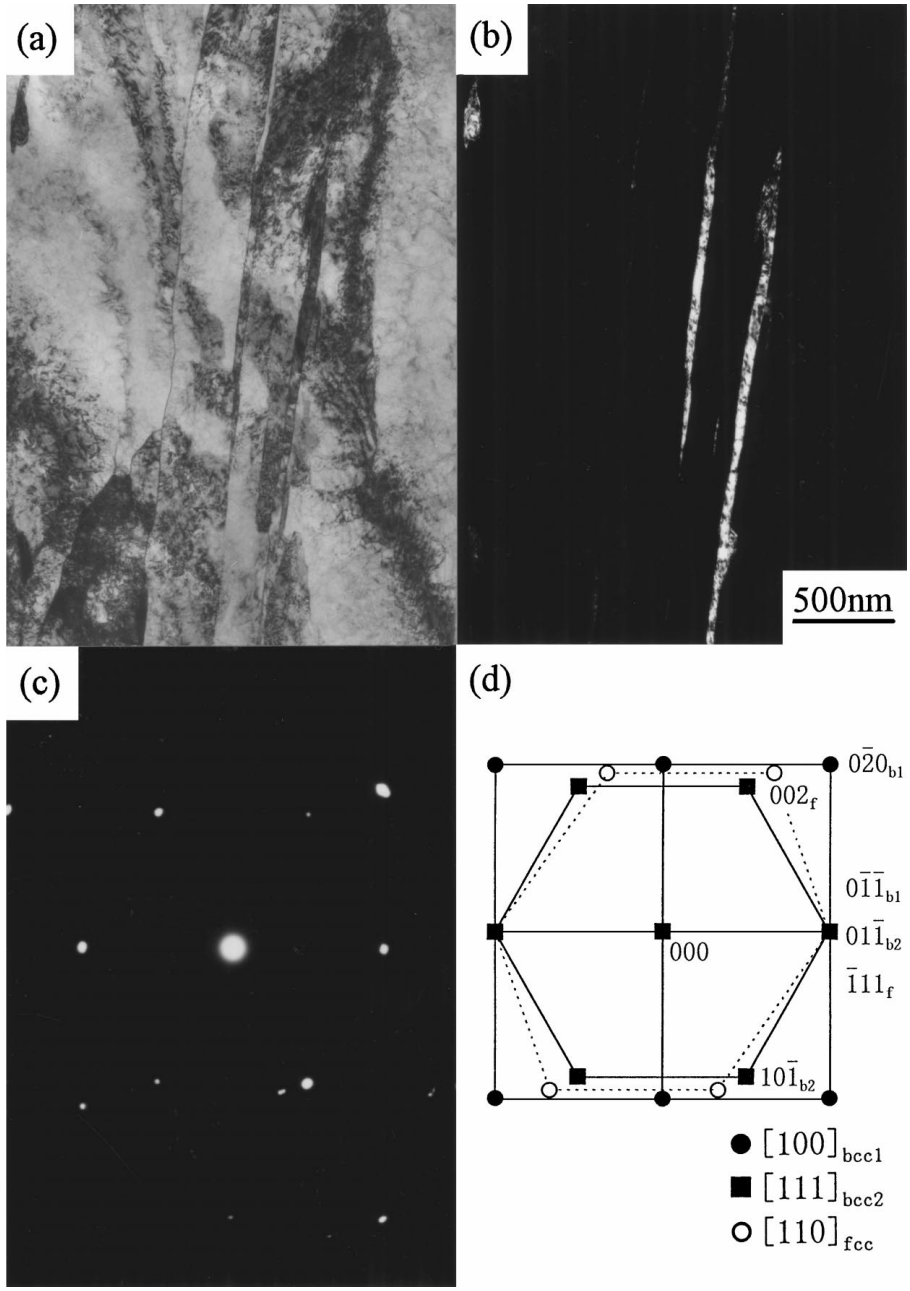

Figure 5 Transmission electron micrographs of the specimen aged at 753 K for 14.4 ks: (a) bright field image, (b) dark field image of austenite, (c) selected area diffraction pattern, and (d) schematic selected area diffraction pattern of (c).

[6–8]. The dark field image (Fig. 5b) taken from γ reflection reveals the interlath films of retained γ. The selected area diffraction pattern (Fig. 5c) consists of three reciprocal lattice sections corresponding to two bcc martensite zones, $[111]_{bcc}$ and $[100]_{bcc}$, and a single fcc γ zone, $[110]_{fcc}$, as shown in Fig. 5d. Therefore, both orientation relationships of Kurdjumov-Sachs ($(01\,\bar{1})_{bcc}//(\bar{1}11)_{fcc}$, $[111]_{bcc}//[110]_{fcc}$) and Nishiyama-Wassermann ($(0\,\bar{1}1)_{bcc}//(\bar{1}11)_{fcc}$, $[100]_{bcc}//[110]_{fcc}$) are found to coexist between the martensite and the interlath γ. Such diffraction pattern has been frequently observed from an area containing lath martensite and interlath γ [9–11]. However, it is difficult only from this result to determine the orientation relationship between the martensite and the interlath γ. It is necessary to perform the accurate measurement of orientation relationship by tilting the specimen to the orientation $[011]_{bcc}//[111]_{fcc}$ as indicated by Sandvik *et al.* [12]. The microstructures of the specimens aged at 813 K and 853 K for 14.4 ks were observed under the same condition, $[110]_{fcc}$ beam direction. The dark field contrasts showing the distribution of γ are shown in Fig. 6. The reversion of martensite to γ can be easily recognized on comparing Fig. 6 with Fig. 3b. Those reverted γ are found to appear parallel to the martensite laths, and such reverted γ has been called lath-like γ [13]. The lath-like γ may mainly grow from the prior interlath retained γ which exists after solution treatment, so that the lamellar duplex microstructure of the γ lath and the aging hardened martensite lath can be formed in each packet. Moreover, there were also Kurdjumov-Sachs or Nishiyama-Wassermann orientation relationship between the γ lath and the martensite lath. Therefore, the orientation relationship can be maintained during the reversion. The twins formed on $\{112\}_{bcc}$ plate, the presence of which is known to reduce its ductility [14],

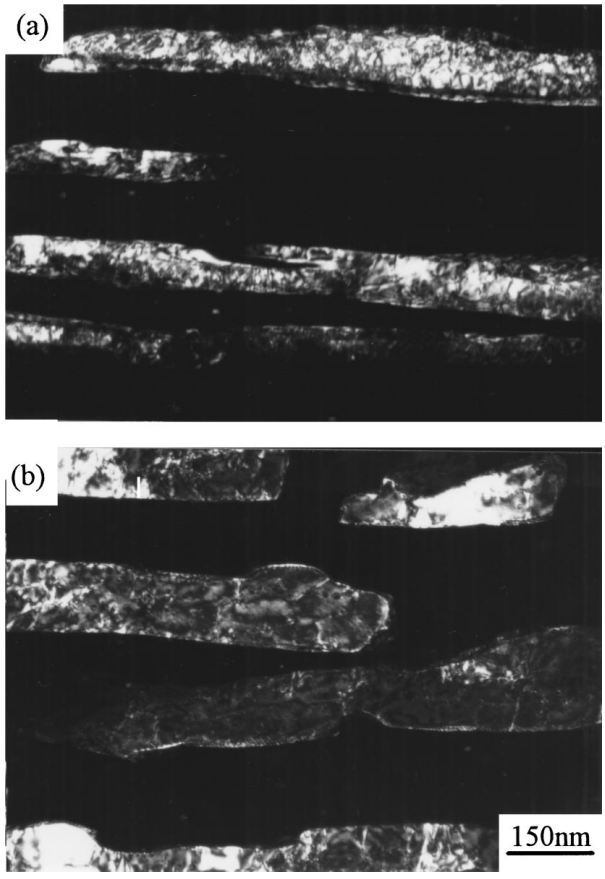

Figure 6 Transmission electron micrographs of the specimens aged at (a) 813 K and (b) 853 K for 14.4 ks.

were observed in all specimens, however, such twin was very low in density.

Fig. 7 shows the transmission electron micrographs of the martensite lath in the specimens aged at 753 K, 813 K and 853 K for 14.4 ks. In the specimen aged at 753 K (Fig. 7a), precipitates can not be clearly observed due to a high density of dislocation. However, smaller precipitates may distribute in the martensite laths, since the increase in hardness is obtained. In the specimens aged at 813 K (Fig. 7b) and 853 K (Fig. 7c), very fine precipitates can be observed on the dislocations. The mean size of precipitates even after aging at 853 K is found to be about 30 nm. Those precipitates were found to be enriched with Cu by means of energy disparsive X-ray spectroscopy equipped in TEM. The precipitates in the specimen aged at 753 K and 813 K are considered to be Cu-rich cluster, while the precipitates in the specimens aged at 853 K may be fcc ε-Cu phase on the basis of those sizes [15]. Laves and σ phases which may exist on equilibrium condition below 840 K as shown in Fig. 1 can not be observed, moreover, carbides and nitrides can not be also observed.

3.3. Mechanical properties

Five kinds of specimens aged at various temperatures in the range 713 K–853 K for 14.4 ks were prepared for the evaluation of mechanical properties. Fig. 8 shows the effect of aging temperature on the tensile properties. Below 773 K, the 0.2% yield strength gradually increases with rising aging temperature, while the tensile strength slightly decreases. On the other hand, the 0.2% yield strength and tensile strength gradually decrease with rising aging temperature above 773 K. As described above, Fig. 3 reveals that the reversion of martensite to γ occurs on aging above 773 K for 14.4 ks. Consequently, the formation of reverted γ may results in the decrease in the 0.2% yield strength and tensile strength above 773 K. On the other hand, the decrease in the tensile strength below 773 K may be caused by the over aging of precipitates. However, the cause of increase in the 0.2% yield strength below 773 K is not clear. The elongation and reduction of area increase with rising aging temperature regardless of aging temperature. X-ray diffraction just under the fracture surfaces of the tensile specimens revealed that there was a few amount of γ in the specimen aged at 853 K only.

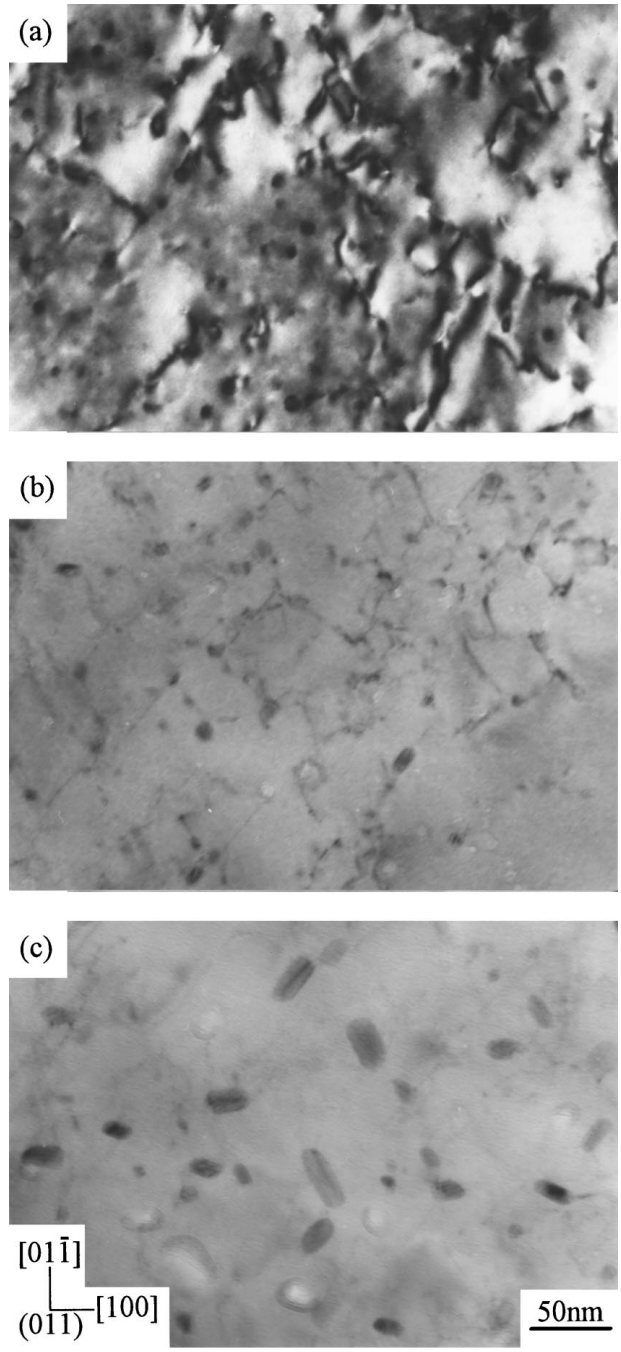

Figure 7 Transmission electron micrographs of the martensite lath of the specimens aged at (a) 753 K, (b) 813 K and (c) 853 K for 14.4 ks.

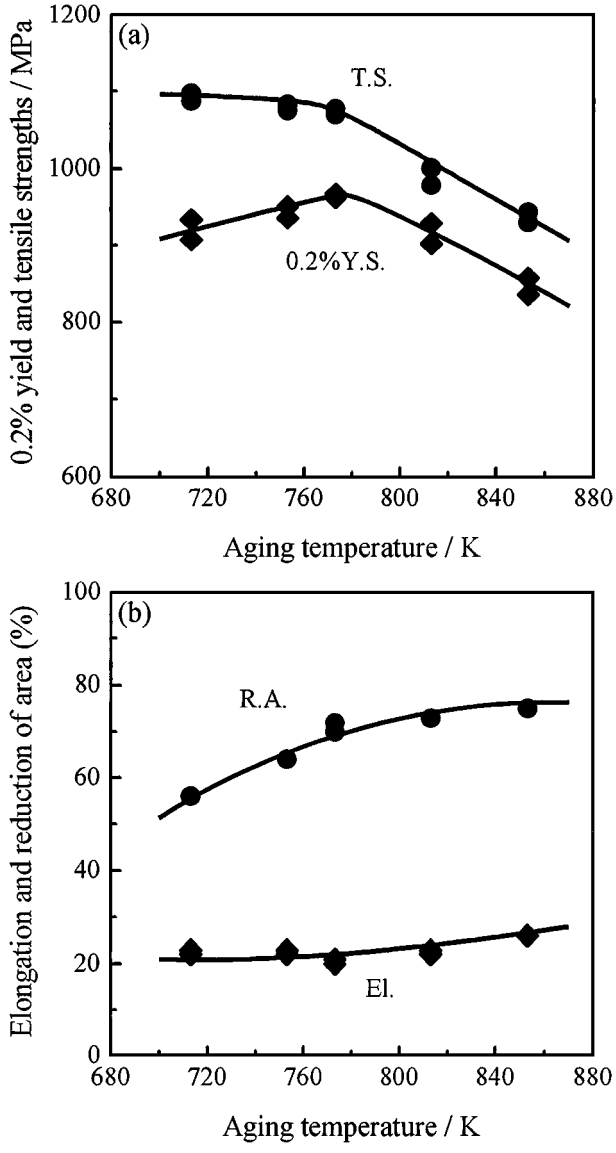

Figure 8 Effects of aging temperature on (a) 0.2% yield and tensile strengths and (b) elongation and reduction of area.

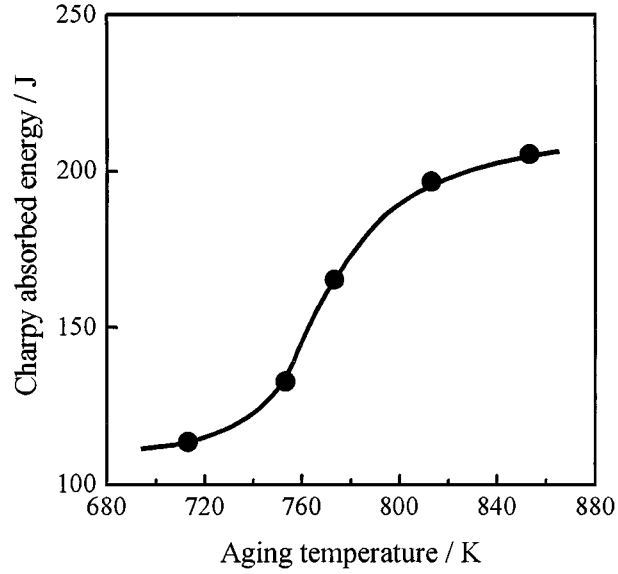

Figure 9 Effects of aging temperature on Charpy V-notch absorbed energy.

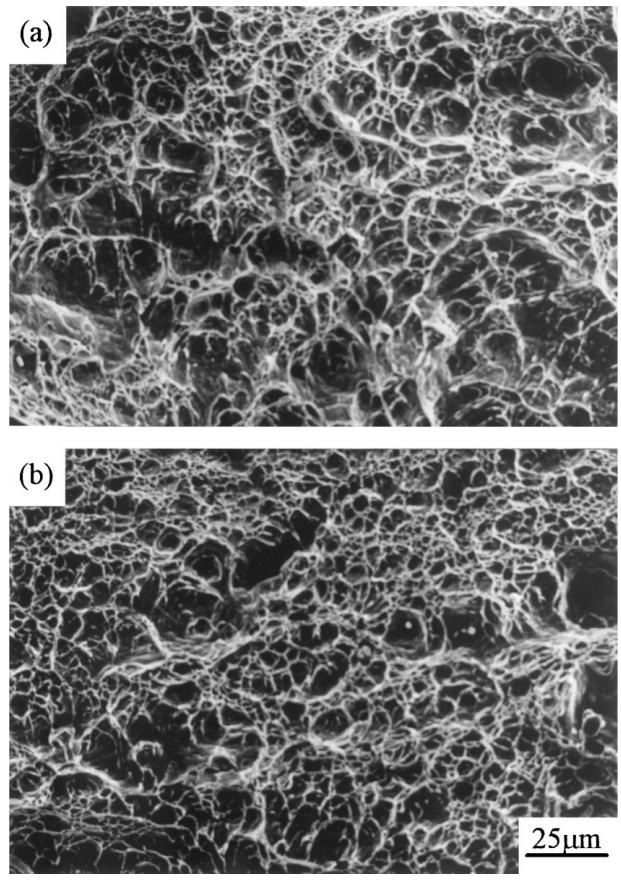

Figure 10 Fractographic features of the Charpy impact specimens aged at (a) 713 K and (b) 773 K for 14.4 ks.

Therefore, almost all of the γ in each specimen may be transformed to martensite during tensile deformation.

Fig. 9 shows the effect of aging temperature on the Charpy V-notch absorbed energy. The Charpy absorbed energy increases with rising aging temperature, and its increase is remarkable at around 773 K. The obtained Charpy absorbed energies are very high values in the range 100–200 J. Some examples of the fractographic feature are shown in Fig. 10. Ductile dimpled fracture can be observed even in the specimen aged at 713 K.

4. Discussion

4.1. Formation process of reverted austenite

In the present steel, the reversion of martensite to γ can be observed on aging above around 773 K as shown in Figs 2b and 3b. This temperature is lower than the temperature at which the reversion is detected in other martensitic precipitation hardening stainless steels [6, 8, 16]. The analysis of the formation process of reverted γ is performed by using the measured γ contents with aging time at 813 K, 833 K and 853 K. Generally, Johnson-Mehl eqution given by Equation 1 can be used to describe the progress of a number of nucleation and growth reactions including diffusion controlled precipitation reaction:

$$y = 1 - \mathrm{e}^{-(kt)^n} \quad (1)$$

where y, t, k and n are the volume fraction transformed, the aging time, constant for a given temperature and

the time exponent, respectively [17, 18]. The time exponent, n, is a useful parameter which provides a semi-quantitative description of the isothermal tranformation kinetics. This parameter is independent of temperature, provided the reaction mechanism dose not change over the range of condition of encountered. The n values have been used for predicting the conditions and morphologies of particular phase changes. Equation 2 can be obtained by taking logarithm of Equation 1:

$$\ln\left(\ln\frac{1}{1-y}\right) = n\ln t + n\ln k \qquad (2)$$

Thus, a plot of $\ln(\ln(1/(1-y)))$ against $\ln t$ should yield a straight line of slop n and intercept $n \ln k$. The plots of the present data revealed that the time exponent, n, for the progress of reversion was found to be about $1/2$ without dependence of aging temperature. Christian has reported that n is $1/2$ on thickening of plate phase by diffusion controlled [18], which is consistent with the microstructure changes as shown in Fig. 6.

The temperature dependence of transformation kinetics can be estimated by the Arrhenius equation given by Equation 3:

$$k = k_0 \exp\left(-\frac{Q}{RT}\right) \qquad (3)$$

where k_0, Q, R and T are constant, the apparent activation energy, ideal gas constant and the absolute temperature, respectively. The k value for each temperature, 813 K, 833 K and 853 K, was calculated from each intercept, $n \ln k$, and then the relationship between $1/T$ and $\ln k$ was obtained in accordance with Equation 3. Fig. 11 shows Arrhenius plot for the formation of reverted γ. Linear correlation is found between $1/T$ and $\ln k$, and the apparent activation energy for the formation of reverted γ in the present steel can be estimated as 240 kJ/mol from the slope of the straight line and is very close to 245 kJ/mol which is the activation energy for diffusion of Ni in ferrite [19]. Consequently, the formation process of reverted γ in the present steel can be rationalized to be controlled by diffusion of Ni in martensite matrix. Since the concentration of Ni in reverted γ has been reported in tempered martensitic steels containing Ni [14, 20–22], it is reasonable that the experimentally obtained apparent activation energy corresponds to the activation energy for diffusion of Ni in ferrite.

For confirming above discussion, the composition changes of martensite and γ with aging time at 853 K were examined by using energy disparsive X-ray spectroscopy equipped in TEM. The concentrations of main four elements, Fe, Cr, Ni and Mo, were analyzed, and the total of concentrations of four elements was estimated as 100 mass%. Cu was excepted from the analysis, because the error become larger due to the precipitation in the martensite. The results of composition analysis are shown in Fig. 12. The following points can be seen in this figure: (1) The composition of the reverted γ dose not change with aging time. (2) Ni content in the reverted γ is about 15 mass% which is twice

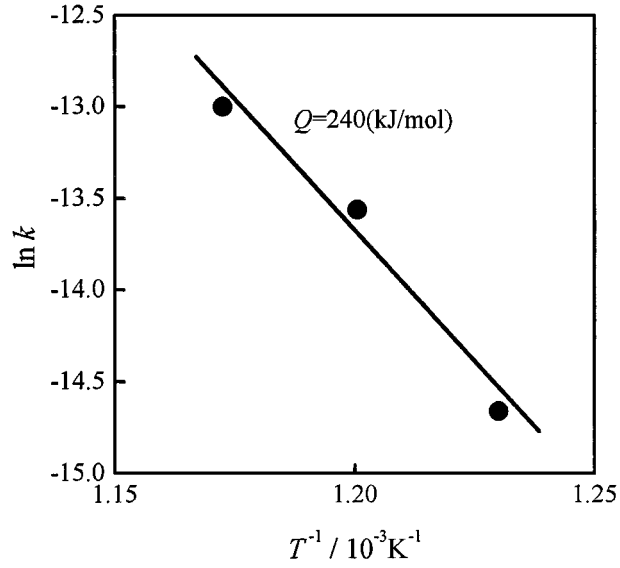

Figure 11 Arrhenius plot for the formation of reverted austenite.

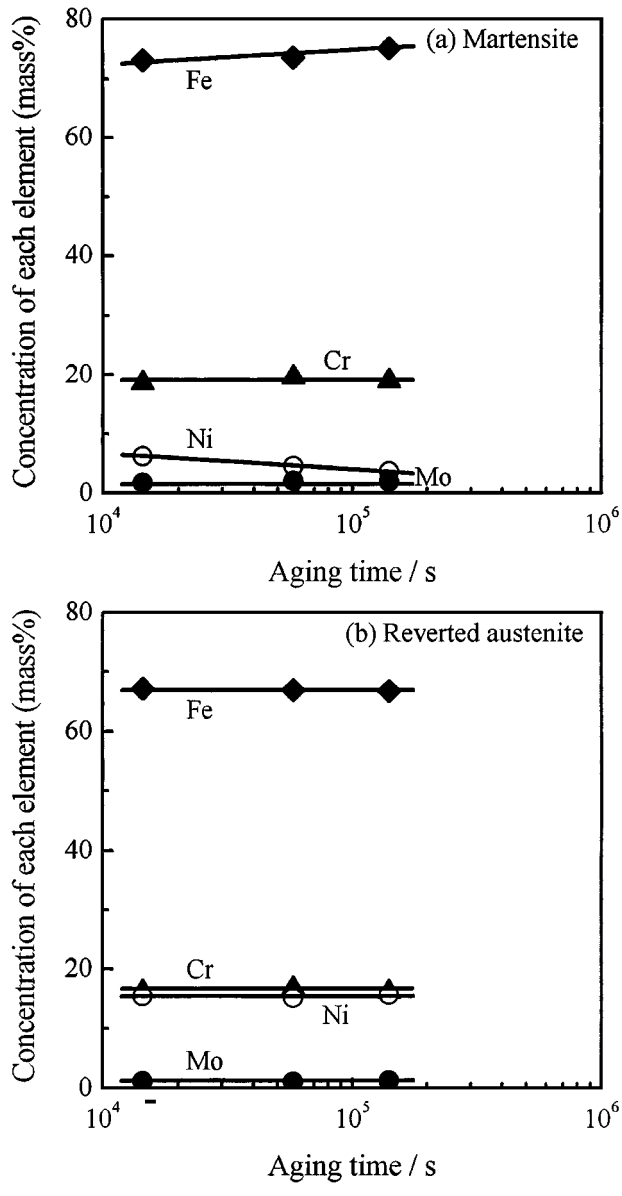

Figure 12 Composition changes of (a) the martensite and (b) the reverted austenite with aging time at 853 K.

that in the steel. (3) The decrease in Ni content and the increase in Fe content with aging time can be seen in the martensite, and other contents dose not change. Consequently, Ni is easily recognized to diffuse to the reverted γ from the martensite during aging, which is consistent with the above discussion about the activation energy. (4) Ni content which is γ former increases in the reverted γ, while Cr content which is ferrite former conversely increases in the martensite. Therefore, C and N which are also γ former may be concentrated to the reverted γ. These tendencies may be applicable to the reversion process at other aging temperatures. Since γ is known to be stabilized with increasing Ni content, the reverted γ involved in the specimen aged above 773 K is more stable than the retained γ involved in the specimen aged below 773 K.

4.2. The combinations of the strength, ductility and toughness

The product of tensile strength by elongation, T.S. $\times$ El., has been often utilized as the index of the balance between strength and ductility. Its value become 24590, 24280, 22009, 22270 and 24362 MPa% for each specimen aged at 713 K, 753 K, 773 K, 813 K and 853 K for 14.4 ks, respectively. These values, which are approximately constant, are found to be higher than that of other martensitic precipitation hardening stainless steels such as 17-4 PH and PH 13-8 Mo stainless steels [1].

Fig. 13 shows the relationship between the tensile strength and the Charpy V-notch absorbed energy of some martensitic precipitation hardening stainless steels [1] and the present steel. The present steel aged at 713 K for 14.4 ks is found to have a combinations of tensile strength and absorbed energy in the same level as PH 13-8 Mo stainless steel, and the combination is found to be improved with rising aging temperature because of remarkable increase in absorbed energy. The present steels aged at 813 K and 853 K for 14.4 ks, in which the reversion of martensite to γ is observed, are found to have both a tensile strength of 1000 MPa grade and a high absorbed energy of 200 J. The remarkable improvement of toughness with the reversion can be attributed to the effective crack arrest mechanism, which is energy absorption due to γ to martensite transformation, in the formed duplex microstructure of the reverted γ and the aging hardened martensite.

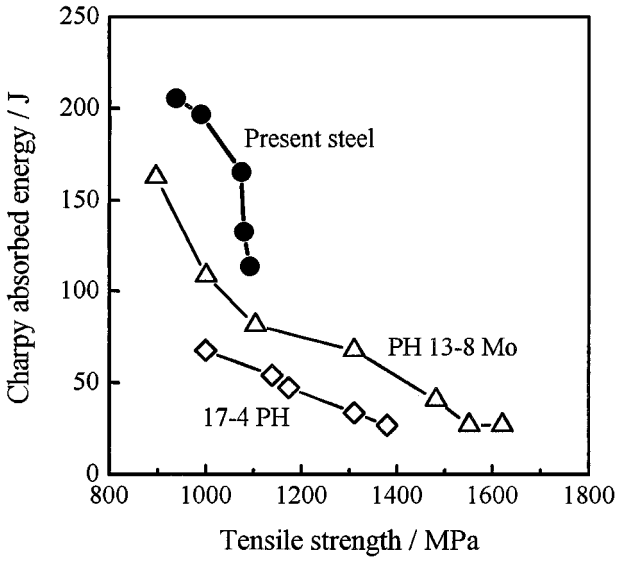

Figure 13 Relationships between the tensile strength and the Charpy V-notch absorbed energy of PH 13-8 Mo and 17-4 PH stainless steels and the present steel.

The reasons for the excellent combinations of strength, ductility and toughness obtained in the present steel containg reverted γ may be as follows: (1) Nonmetallic inclusions and impurities were minimized. (2) The δ-ferrite dose not remain after solution treatment. (3) Carbides and nitrides can not be observed in the specimen aged below 853 K. (4) About 12% γ remains after solution treatment. (5) The twins formed on $\{112\}_{bcc}$ plate were very low in density. (6) The reverted γ is formed during aging above 773 K which is relatively low temperature. (7) The reverted γ may mainly grow from the prior interlath retained γ which exists after solution treatment, so that the lamellar duplex microstructure of the reverted γ and the aging hardened martensite can be formed in each packet, and the interface between those two phases have good coherency.

5. Conclusion

In the present work, the effects of aging temperature on the microstructure and mechanical properties of a newly designed martensitic precipitation hardening stainless steel, which is 1.8Cu-15.9Cr-7.3Ni-1.2Mo-low C, N steel, were experimentally investigated. The main results are as follows:

1. Hardness changes of the present steel with aging time may depend on the balance between the softening due to the reversion and the hardening due to the precipitation. The maximum hardness can be obtained in the specimen aged at around 693 K.
2. The specimen aged at 753 K for 14.4 ks has a typical lath martensitic structure with about 12% interlath γ. On the other hand, the specimens aged at 813 K and 853 K for 14.4 ks have the lamellar duplex microstructure of the reverted γ and the aging hardened martensite.
3. The formation process of reverted γ is controlled by diffusion of Ni in martensite, and Ni concentrate in the reverted γ. The chemical composition of the reverted γ dose not change with aging time.
4. In the specimens aged at 753 K, 813 K and 853 K for 14.4 ks, the mean size of precipitates which are enriched with Cu increases with rising aging temperature, however, it is about 30 nm even after aging at 853 K.
5. The specimens aged at 813 K and 853 K for 14.4 ks, in which the reversion of martensite to γ is observed, have the excellent combinations of strength, ductility and toughness.

References

1. D. PECKNER and I. M. BERNSTEIN, "Handbook of Stainless Steel" (McGraw-Hill Book Co., New York, 1977) p. 7.13, 20.32.
2. H. NAKAGAWA and T. MIYAZAKI, *J. Mater. Sci.* submitted.

3. B. SUNDMAN, B. JANSSON and J. O. ANDERSSON, *CALPHAD* **9** (1985) 153.
4. M. HILLERT and C. QUI, *Metall. Trans. A* **21A** (1990) 1673.
5. M. J. DICKSON, *J. Appl. Cryst.* **2** (1969) 176.
6. V. SEETHARAMAN, M. SUNDARARAMAN and R. KRISHNAN, *Mater. Sci. Eng.* **47** (1981) 1.
7. T. MAKI, H. MORIMOTO and I. TAMURA, *Trans. ISIJ* **20** (1980) 700.
8. U. K. VISWANATHAN, S. BANERJEE and R. KRISHNAN, *Mater. Sci. Eng.* **A104** (1988) 181.
9. B. V. N. RAO, *Metall. Trans. A* **10A** (1979) 645.
10. G. THOMAS, *ibid.* **9A** (1978) 439.
11. Y. KATZ, H. MATHIAS and S. NADIV, *ibid.* **14A** (1983) 801.
12. B. P. J. SANDVIK and C. M. WAYMAN, *ibid.* **14A** (1983) 809.
13. L. T. SHIANG and C. M. WAYMAN, *Metallography* **21** (1988) 425.
14. S. J. KIM and C. M. WAYMAN, *Mater. Sci. Eng.* **A128** (1990) 217.
15. P. J. OTHEN, M. L. JENKINS and G. D. W. SMITH, *Phil. Mag. A* **70** (1994) 1.
16. W. M. GARRISON, JR. and J. A. BROOKS, *Mater. Sci. Eng.* **A149** (1991) 65.
17. J. BURKE, "The Kinetics of Phase Transformations in Metals" (Pergamon Press Ltd., Oxford, 1965) p. 36.
18. J. W. CHRISTIAN, "The Theory of Transformations in Metals and Alloys" (Pergamon Press Ltd., Oxford, 1965) p. 475.
19. K. HIRANO, M. COHEN and B. L. AVERBACH, *Acta Metall.* **9** (1961) 440.
20. W. SHA, A. CEREZO and G. D. W. SMITH, *Metall. Trans. A* **24A** (1993) 1221.
21. G. R. SPEICH, *Trans. Met. Soc. AIME* **227** (1963) 1436.
22. P. P. SINHA, D. SIVAKUMAR, N. S. BABU, K. T. THARIAN and A. NATARAJAN, *Steel Res.* **66** (1995) 490.

Received 26 January
and accepted 11 August 1999